Review of high-throughput approaches to search for piezoelectric nitrides

Kevin R. Talley,[1,2] Rachel Sherbondy,[1,2] Andriy Zakutayev,[2] and Geoff L. Brennecka[1,a)]
[1]*Department of Metallurgical and Materials Engineering, Colorado School of Mines, 1500 Illinois St, Golden, Colorado 80401*
[2]*Materials Science Center, National Renewable Energy Laboratory, 15013 Denver West Pkwy, Golden, Colorado 80401*

(Received 24 August 2019; accepted 7 October 2019; published 24 October 2019)

Piezoelectric materials are commonplace in modern devices, and the prevalence of these materials is poised to increase in the years to come. The majority of known piezoelectrics are oxide materials, due in part to the related themes of a legacy of ceramists building off of mineralogical crystallography and the relative simplicity of fabricating oxide specimens. However, diversification beyond oxides offers exciting opportunities to identify and develop new materials perhaps better suited for certain applications. Aluminum nitride (and recently, its Sc-modified derivative) is the only commercially integrated piezoelectric nitride in use today, although this is likely to change in the near future with increased use of high-throughput techniques for materials discovery and development. This review covers modern methods—both computational and experimental—that have been developed to explore chemical space for new materials with targeted characteristics. Here, the authors focus on the application of computational and high-throughput experimental approaches to discovering and optimizing piezoelectric nitride materials. While the focus of this review is on the search for and development of new piezoelectric nitrides, most of the research approaches discussed in this article are both chemistry- and application-agnostic. https://doi.org/10.1116/1.5125648

I. INTRODUCTION TO PIEZOELECTRICS AND NITRIDES

Integrated piezoelectrics have become ubiquitous in modern life, converting electrical energy to mechanical energy and vice versa behind the scenes in applications ranging from wireless communications and inkjet printers to medical ultrasound. For the first century after the discovery of the piezoelectric effect in 1880,[1] the vast majority of piezoelectrics were based on α-quartz, $BaTiO_3$, or $Pb(Zr, Ti)O_3$. In recent decades, both demand for new applications and availability of new materials fabrication and integration technologies have led to a rapid expansion in the piezoelectric materials space, fueled in part by the desire to develop lead-free piezoelectric materials with properties comparable to $Pb(Zr, Ti)O_3$.[2]

In parallel, nitride materials have also established themselves as essential components of modern technology. Led by flagship GaN-based semiconductors, these materials have revolutionized the field of energy-efficient lighting.[3] In addition, nitride based materials are commonly used for hard coatings,[4] catalysis,[5] and many other applications. These technological successes refueled interest to design and discover new functional materials in a broader family of nitrides.

In recent years, high-throughput techniques have massively increased the rate of materials discovery and development. Ever-increasing computational power enables high-throughput computation of properties for all pure chemical compounds with known crystal structures. Similarly, increased automation of experimental equipments has led to significant increases in throughput of materials experimentation. Finally, paired computational and experimental methods coupled to data mining and machine learning for materials discovery have benefited greatly from investment fueled by the Materials Genome Initiative (MGI).

The present article summarizes the intersection of these three topics, briefly reviewing high-throughput studies of piezoelectrics and nitrides more generally before focusing on recent efforts for the rapid discovery and development of new piezoelectric nitrides. To this end, we begin by discussing piezoelectric materials properties (Sec. I A) and nitride materials (Sec. I B) rather broadly. We then present a detailed discussion of the efforts and strategies used to identify new piezoelectric materials by both theory (Sec. II) and high-throughput experimental (Sec. III) approaches, and then focus on how these two approaches are used in conjunction for the study of piezoelectric nitrides specifically (Sec. IV). Finally (Sec. V), we suggest strategies for the continued exploration of the nitride piezoelectric materials space.

A. Piezoelectric materials

Piezoelectric ceramics have many industrial uses in bulk form including micropositioners, actuators, and ultrasonic motors.[6] They are equally useful as thin films in applications such as energy harvesting,[7] microelectromechanical systems (MEMS),[8] acoustic devices,[9] transducers,[10] and lab-on-a-chip devices.[11] The field of piezoMEMS devices has emerged as particularly vibrant, both technologically and economically, for various types of sensors, actuators, and filters.[12] In these devices, the active piezoelectric layer is typically one of the materials in Tables I and II depending on the device

a)Electronic mail: geoff.brennecka@mines.edu

TABLE I. Relative dielectric permittivity at constant strain (ϵ_{33}^{χ}) and stress (ϵ_{33}^{σ}), the independent piezoelectric strain coefficients (d_{33}, d_{31}, d_{15}), the mechanical quality factor (Q_m), mechanical coupling coefficient (k_{33}), pyroelectric coefficient (ρ), two mechanical compliance coefficients at constant electric field (S_{11}^{E}, S_{33}^{E}), and the piezoelectric Curie temperature (T_C) for common materials, including two nitrides [gallium nitride and aluminum nitride (AlN)], two oxides (zinc oxide and silicon dioxide), and one sulfide (cadmium sulfide). Values are reproduced from C. R. Bowen, H. A. Kim, P. M. Weaver, and S. Dunn, Energy Environ. Sci. **7**, 25 (2014)[7] by permission of The Royal Society of Chemistry, T_C values added here.

Material	GaN	AlN	CdS	ZnO	α-(SiO_2)
Piezoelectric	✓	✓	✓	✓	✓
Pyroelectric	✓	✓	✓	✓	✗
Ferroelectric	✗	✗	✗	✗	✗
ϵ_{33}^{χ}	11.2 (Ref. 13)	10 (Ref. 14)	9.53 (Ref. 15)	8.84 (Ref. 16)	4.63 (Ref. 17)
ϵ_{33}^{σ}	…	11.9 (Ref. 18)	10.33 (Ref. 15)	11.0 (Ref. 16)	4.63 (Ref. 17)
d_{33} (pC/N)	3.77 (Ref. 19)	5 (Ref. 19)	10.3 (Ref. 15)	12.4 (Ref. 20)	$d_{11} = -2.3$ (Ref. 17)
d_{31} (pC/N)	−19 (Ref. 19)	−2 (Ref. 19)	−5.18 (Ref. 15)	−5.0 (Ref. 20)	…
d_{15} (pC/N)	3.1 (Ref. 21)	3.6 (Ref. 21)	−13.98 (Ref. 15)	−8.3 (Ref. 20)	$d_{14} = 0.67$ (Ref. 17)
Q_m	2800 (Ref. 22)	2490 (Ref. 12)	1000 (Ref. 23)	1770 (Ref. 12)	10^5–10^6 (Ref. 24)
k_{33}	…	0.23 (Ref. 12)	0.26 (Ref. 15)	0.48 (Ref. 20)	0.1 (Ref. 25)
ρ [μC/(m^2 K)]	−4.8 (Ref. 26)	−(6–8) (Ref. 27)	−4 (Ref. 28)	−9.4 (Ref. 28)	…
S_{11}^{E} (10^{-12}/Pa)	3.326 (Ref. 29)	2.854 (Ref. 29)	20.69 (Ref. 30)	7.86 (Ref. 30)	12.77 (Ref. 17)
S_{33}^{E} (10^{-12}/Pa)	2.915 (Ref. 29)	2.824 (Ref. 29)	16.97 (Ref. 30)	6.94 (Ref. 30)	9.73 (Ref. 17)
T_C (°C)	>1000 (Ref. 31)	>2000 (Ref. 32)	>1000 (Ref. 33)	>2000 (Ref. 34)	573 (Ref. 35)

requirements and the fabrication facility capabilities.[12] The first three rows of each table show the existence of piezoelectric, pyroelectric, and/or ferroelectric properties. These classifications are determined by the symmetry of the material, which is represented graphically in Fig. 1(b).

Piezoelectric materials exhibit a crystalline symmetry that is noncentrosymmetric (lacking an inversion center) such that the application of a mechanical stress results in the separation of charge centers and development of an electric dipole. Conversely, the application of an electric field produces a mechanical strain. The electrical and mechanical properties of piezoelectrics are, therefore, intimately coupled. To be piezoelectric, the material must belong to one of 20 noncentrosymmetric crystal classes:[47] 1, 2, m, 222, mm2, 4, $\bar{4}$, 422, 4mm, $\bar{4}$2m, 3, 32, 3m, 6, $\bar{6}$, 622, 6mm, $\bar{6}$2m, 23, or $\bar{4}$3m. Further, materials belonging to one of the 10 polar crystal classes[47] (1, 2, m, mm2, 4, 4mm, 3, 3m, 6, 6mm) possess a permanent ("spontaneous") dipole at the unit cell level even in the absence of an external electric field. As the magnitude of this spontaneous dipole is naturally temperature-dependent, these materials are referred to as pyroelectric. Ferroelectric materials are an experimental subset of pyroelectric materials in which the direction of the permanent dipole can be reversibly reoriented under an external electric field.

Piezoelectrics, therefore, couple mechanical and electrical energy through noncentrosymmetric symmetry at the

TABLE II. Relative dielectric permittivity at constant strain (ϵ_{33}^{χ}) and stress (ϵ_{33}^{σ}), the independent piezoelectric strain coefficients (d_{33}, d_{31}, d_{15}), the mechanical quality factor (Q_m), mechanical coupling coefficient (k_{33}), pyroelectric coefficient (ρ), two mechanical compliance coefficients at constant electric field (S_{11}^{E}, S_{33}^{E}), and the ferroelectric Curie temperature (T_C) for common perovskite structured oxide materials including two classic materials (barium titanate and lithium niobate), "hard" and "soft" $Pb(Zr/Ti)O_3$ materials (PZT-4 and PZT-5H, respectively) and another common alloy system $Pb(Mg_{1/3}Nb_{2/3})O_3 - PbTiO_3$ (PMN-PT). Values are reproduced from C. R. Bowen, H. A. Kim, P. M. Weaver, and S. Dunn, Energy Environ. Sci. **7**, 25 (2014)[7] by permission of The Royal Society of Chemistry, T_C values added here.

Material	$BaTiO_3$	PZT-4	PZT-5H	PMN-PT	$LiNbO_3$
Piezoelectric	✓	✓	✓	✓	✓
Pyroelectric	✓	✓	✓	✓	✓
Ferroelectric	✓	✓	✓	✓	✓
ϵ_{33}^{χ}	910 (Ref. 36)	635 (Ref. 36)	1470 (Ref. 36)	680 (Ref. 37)	27.9 (Ref. 38)
ϵ_{33}^{σ}	1200 (Ref. 36)	1300 (Ref. 36)	3400 (Ref. 36)	8200 (Ref. 37)	28.7 (Ref. 38)
d_{33} (pC/N)	149 (Ref. 36)	289 (Ref. 36)	593 (Ref. 36)	2820 (Ref. 37)	6 (Ref. 38)
d_{31} (pC/N)	−58 (Ref. 36)	−123 (Ref. 36)	−274 (Ref. 36)	−1330 (Ref. 37)	−1.0 (Ref. 38)
d_{15} (pC/N)	242 (Ref. 36)	495 (Ref. 36)	741 (Ref. 36)	146 (Ref. 37)	69 (Ref. 24)
Q_m	400 (Ref. 36)	500 (Ref. 36)	65 (Ref. 36)	43–2050 (Refs. 12 and 39)	10^4 (Ref. 40)
k_{33}	0.49 (Ref. 41)	0.7 (Ref. 42)	0.75 (Ref. 42)	0.94 (Ref. 37)	0.23 (Ref. 24)
ρ [μC/(m^2 K)]	−200 (Ref. 28)	−260 (Ref. 28)	−260 (Ref. 28)	−1790 (Ref. 43)	−83 (Ref. 28)
S_{11}^{E} (10^{-12}/Pa)	8.6 (Ref. 36)	12.3 (Ref. 36)	16.4 (Ref. 36)	69.0 (Ref. 37)	5.83 (Ref. 38)
S_{33}^{E} (10^{-12}/Pa)	9.1 (Ref. 36)	15.5 (Ref. 36)	20.8 (Ref. 36)	119.6 (Ref. 37)	5.02 (Ref. 38)

crystallographic unit cell level such that application of a mechanical stress produces a surface charge on an insulating piezoelectric. This relationship between applied stress (σ_{ij}) and dielectric displacement (D_i) is the direct piezoelectric effect [Eq. (1)], while an applied electric field (E_i) produces mechanical strain (χ_{ij}) via the converse piezoelectric effect [Eq. (2)]. Both responses are governed by the piezoelectric strain coefficient (d_{ijk}). Piezoelectric materials are often characterized by the piezoelectric stress coefficient (e_{ijk}), elastic stiffness or compliance (c_{ijkl} or s_{ijkl}), piezoelectric strain coefficient (d_{ijk}), and dielectric permittivity (ϵ_{ij}), which are all tensor values, reflecting the anisotropy common in crystalline materials. The relationships among these values are shown schematically in Fig. 1 and described in the equations that follow using reduced (Voigt) notation for simplicity. Derivation of these relationships and further details on the reduced tensor notation used within can be found elsewhere.[46,48] It should also be noted that the equations outlined below and Fig. 1 assume that all other parameters (e.g., temperature, magnetic field, and so on) are constant; extension of the concepts to additional coupled phenomena is straightforward.[46,49]

The electrical properties of a polarizable deformable solid are related to the mechanical properties through the the piezoelectric coefficients [Eqs. (1) and (2)],

$$D_i = e_{ik}\chi_j \quad \text{or} \quad D_i = d_{ik}\sigma_k, \tag{1}$$

$$\chi_i = d_{ik}E_k \quad \text{or} \quad \sigma_i = -e_{ik}E_j. \tag{2}$$

Each of these relationships can be written in terms of the strain (χ_k) or stress (σ_k) fields, as the piezoelectric coefficients d_{ik} and e_{ik} are connected through the mechanical properties of the lattice [Eq. (3)] as shown in Eq. (4),

$$\sigma_i = c_{ik}\chi_k \quad \text{or} \quad \chi_i = s_{ik}\sigma_k, \tag{3}$$

$$d_{ik} = e_{ip}c_{pk} \quad \text{or} \quad e_{ik} = d_{ip}s_{pk}. \tag{4}$$

The standard set of constitutive equations which govern piezoelectric behavior can be derived by combining Eq. (4) with Eq. (1), resulting in Eq. (5) for the total dielectric displacement, and by adding Eqs. (2) and (3), resulting in Eq. (6), which describes the total stress or strain,

$$D_i = \epsilon_{ik}E_k + e_{ik}\chi_k \quad \text{or} \quad D_i = \epsilon_{ik}E_k + d_{ik}\sigma_k, \tag{5}$$

$$\sigma_i = c_{ik}\chi_k - e_{ik}E_k \quad \text{or} \quad \chi_i = s_{ik}\sigma_k + d_{ik}E_k. \tag{6}$$

Thus, piezoelectric performance depends largely on the piezoelectric stress (e_{ik}) and lattice stiffness (s_{ik}). Note that ferroelectricity is not a requirement for piezoelectricty, however, the best known piezoelectrics are usually also ferroelectrics due to strain contributions from domain reorientation.

Strongly coupled structure-property relationships within piezoelectric materials drive research of the corresponding parameters and the tunability of each. One such parameter is the Curie temperature (T_C), which is the temperature at which the material undergoes a transition to a centrosymmetric phase and thus a loss of piezoelectric properties, or from a polar phase to a nonpolar phase and thus a loss of ferroelectric properties, and, therefore, acts as an upper temperature boundary in applications. Most commonly used piezoelectric materials have a T_C in the range of $100 - 500\,^{\circ}\mathrm{C}$ with a few exceptions such as $LiNbO_3$, where $T_C > 1000\,^{\circ}\mathrm{C}$; however there is typically a decrease in piezoelectric performance parameters with increased T_C.[50] See Tables I and II for a comparison of T_C and many other properties mentioned here.

Another structural phenomenon that is frequently used to drive piezoelectric materials development is the morphotropic phase boundary (MPB), which is exemplified in the $Pb(Zr, Ti)O_3$ system. An MPB occurs when there is a (in practice, approximately) temperature-independent phase transition at a specific (or, commonly across a narrow region of) composition. Polarization-dependent properties such as permittivity, piezoelectric coefficients, and ferroelectric response are typically maximized at an MPB due in part to lattice softening and decreased energy barrier for the reorientation of any spontaneous polarization that may be present.

The greater piezoelectric community working on materials which exhibit MPBs have been largely focused on oxide

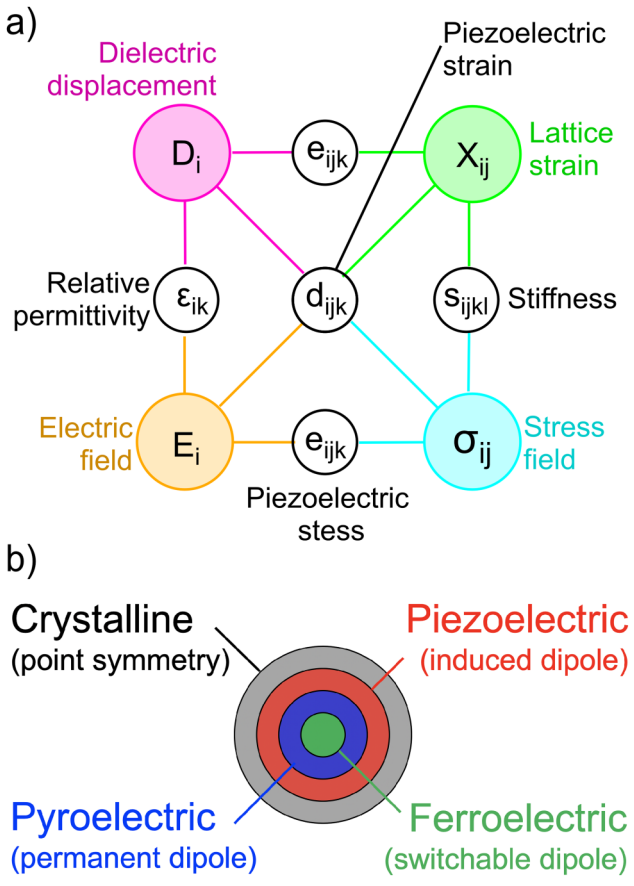

FIG. 1. (a) Partial Heckmann diagram showing the relationships used to describe electrical field and stress coupling in materials, where energy is stored in dielectric displacement and lattice strain. Note: Subscripts are shown here in full form; the rest of this work uses reduced notation (Ref. 46). (b) Nested diagram of categorical descriptors for piezoelectric materials.

materials, but the success of AlN-based alloys has spurred increased interest in the exploration of other nonoxides for use in the thin film form.

B. Nitride materials

Nitrides are an important and growing class of materials exhibiting a variety of useful electronic and physical properties.[51–53] Nitrides have a lower exothermic energy of formation when compared to oxides with a 2:1 nitrogen to oxygen bond energy ratio.[54] In most of the III-nitride materials, there is a strong covalent bond character; however, in other binary nitrides, there is metallic bond character, suggesting ternary nitrides likely contain a wide range of bond character. This results in metal-metal orbital overlap strongly influencing stability and properties.[55] Additionally, it is well known (though often ignored) that many of the computationally-efficient approximations used for high-throughput calculations consistently produce larger deviations from experiments for nitride compounds than for oxides, again reinforcing the importance of tight coupling of computation and experiments. For this review, we limit discussion to studies of nitride materials that show piezoelectric response. Much of the work on piezoelectric properties of nitrides has actually focused on mitigating rather than enhancing piezoelectric effects, such as in the case of multilayer quantum well devices incorporating the AlN–GaN–InN isostructural wurtzite alloy. AlN–GaN–InN is one of the most used nitride systems underlying a wide variety of optoelectronic and power electronic devices.[56] AlN–GaN–InN alloys are flexible, as they can be grown by many methods[57] with a wide lattice constant (4.4–5.0 Å) and bandgap (1.9–6.2 eV) range.[56] The polar character of these materials in relation to lighting and high power/frequency devices has been well documented and reviewed elsewhere.[58,59] In many devices based on this material system, the strain present at heterostructural interfaces requires mitigation (or at least consideration) of the piezoelectric effect because the piezoelectric fields can have substantial effects on the electronic properties of quantum well devices.[57,58,60–62] Piezoelectric properties of AlN and GaN can be compared to other materials in Tables I and II.

The most notable piezoelectric nitride material used in commercial applications is AlN. Even though the piezoelectric strain coefficient is significantly lower than other commercially important piezoelectric materials ($d_{33,\mathrm{AlN}} = 3 - 5\,\mathrm{pm/V}$),[63,64] AlN is utilized for acoustic resonators, primarily for the ease of deposition by physical vapor deposition (PVD) techniques, high mechanical quality factor (Q_m), a near zero temperature dependence of frequency coefficient, and compatibility with complementary metal oxide semiconductor (CMOS) processing facilities.[65] As of the last decade, AlN based alloys have become the focus of many studies for their promise of improved performance.

The nitride chemical space remains under-explored, but this is gradually changing. As shown in Fig. 2, interest within the scientific community in nitride materials, including semiconducting and piezoelectric nitrides, has been steadily increasing over the past 25 years. A substantial amount of piezoelectric nitride literature has focused on better understanding

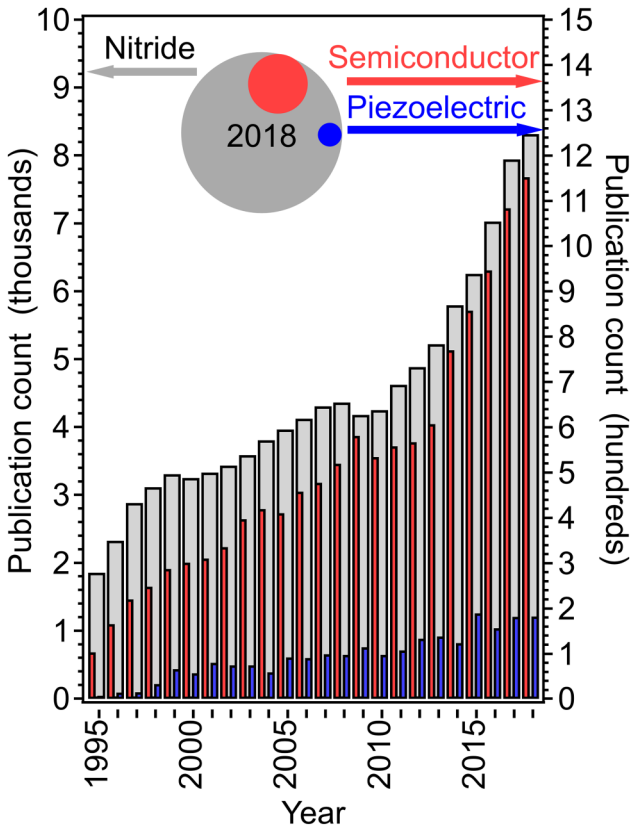

FIG. 2. Number of publications by year under the topic of nitride (gray, left) and under both topics nitride and piezoelectric (blue, right) or nitride and semiconductor (red, right). The inset shows overlap and relative quantities for 2018. Retrieved from Clarivate Analytics Web of Science, May 2019.

the physical parameters, specifically piezoelectric and elastic properties, of aluminum nitride.[66,67] The piezoelectric nitride literature has grown significantly more diverse after reports of enhanced piezoelectric properties in AlN upon alloying with scandium nitride[68] spurred interest in materials beyond AlN.

II. THEORETICAL METHODS FOR DISCOVERING AND UNDERSTANDING PIEZOELECTRICS

Before delving into the development of new piezoelectric nitrides, it is important to briefly review computational approaches from the broader oxide piezoelectric community that have informed the more recent nitride-focused studies. The concepts and strategies of piezoelectric materials modeling are indifferent to the chemistry and only vary by the specific details of the models themselves. While the focus of this review is on piezoelectric nitrides, numerous studies of piezoelectric materials have focused historically on oxide materials. While not nitrides, the principles used within these studies are applicable to nitride materials as well.

The most common tool used for investigating materials through first-principles is density functional theory (DFT). DFT tools have been under development for more than half a century and are now sufficiently accurate (and rapid) to enable exploration of various material parameters and properties computationally, greatly accelerating materials discovery.[69–71] DFT is built around the use of functionals to approximate the

spatially-dependent electron density. Many such functionals have been developed,[72–74] but the selection of the most appropriate functional for a particular calculation is beyond the scope of this review. Modern computational studies have many tools for implementing DFT-based experiments, such as well-developed programs for computing DFT-based models,[75] algorithms for generating random alloy structures,[76] and methods for identifying structural polymorphs.[77]

Computational work can be an important accelerator for experimental learning cycles and vice versa if the information can be shared effectively among researchers. The accessibility and open pipeline for sharing of data is a crucial outcome of the MGI, as it greatly enhances the efficiency of high-throughput experimentation (HTE) in materials science research.[78] Computational investigations are becoming easily available for the experimentalist to access, reuse, and employ as guidance through various open-access databases. These databases come in various flavors: some are diverse and contain results pertinent to many applications,[79,80] some are application specific (such as piezoelectric materials[81]), and some contain experimental results.[82,83]

A. Screening and searching

Theory is commonly leveraged as a method of screening chemical composition space to identify (and/or prioritize) compounds for further exploration with experimental approaches. This approach requires a significant effort and computational resources; however, the time and energy required is a small fraction of that required to screen vast chemical and processing spaces experimentally. Using this approach, researchers calculate and screen material attributes identified as influential in systems with desirable performance.

The general DFT-based approach for building materials understanding begins with computing energetics, properties, and in some instances proxy values used for properties, across optimized structural variations. This data set is then mined for valuable insights capable of informing future selection and optimization within the applicable material space. A representative DFT work flow is presented in Fig. 3 for a chemical screening of the ABX_3 perovskite space which identified 71 possible inorganic perovskites not yet experimentally reported, returning a single nitride.[84] A similar approach focused on nitride (ABN_3) compounds and applied a different set of down selection criteria to find 3 stable perovskites (shown in Fig. 10 and discussed in Sec. IV B). Another example is the use of DFT to examine the oxide perovskite chemical space (ABO_3) for high-performance piezoelectric candidate materials. By investigating the energy associated with structural distortions induced by piezoelectric strain, displacement coupling between the A and B sublattices, the magnitude of spontaneous polarization, density of electronic states for bandgap approximation, and Born effective charges, this study identified 49 candidate piezoelectric materials from a initial set of 3969 possible compositions.[85] Similar approaches have been used on nonoxide perovskite chemistries (ABX_3, $X \neq O$)[84,86] and other crystal systems, such as Half-Heusler structures,[87] all of which identified nitride

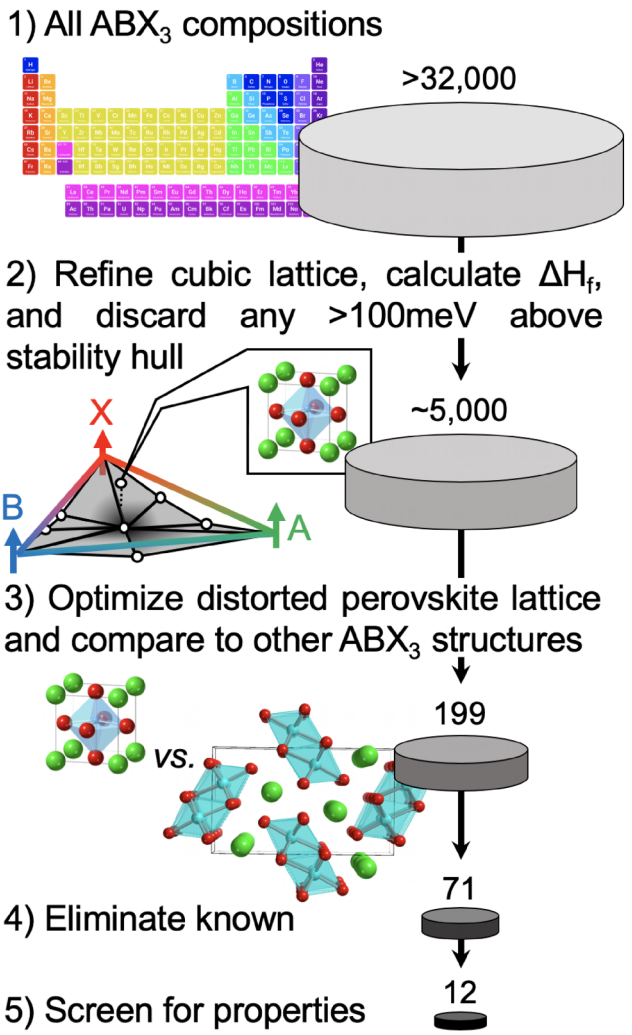

FIG. 3. Representative density functional theory work flow used for screening ABX_3 inorganic perovskites in Ref. 84. (1) Starting with every possible monoatomic ABX_3 compound down selection was done by (2) limiting the the energy of formation difference from the cubic perovskite and the ternary thermodynamic hull of stability, (3) removing compounds favoring a non-perovskite structure, (4) removing experimentally reported compounds, (5) followed by the screening of calculated materials properties. Here, the process distilled 12 new ABX_3 perovskites with promising piezoelectric or ferroelectric indicators.

candidates. While focused on exploring ternary nitrides, recent work[53] builds methodology for high-throughput screening of large chemical spaces for stable and metastable materials, illuminating more than 200 stable and >400 unreported metastable $A_xB_yN_z$ materials. These studies highlight the power of pairing high-throughput screening with an under-explored chemical space like nitrides.

B. Understanding

Once a system has been identified experimentally for notable piezoelectric properties, it is common for a theory-based investigation to follow as a method of understanding the mechanisms which are attributed to the piezoelectric performance.[88,89] Such a computational study can be as simple as calculation of the piezoelectric strain tensor (d_{ij}) from first principles, as demonstrated for the AlN–GaN–InN III-V

nitiride family[90] or as complex as computational investigation of piezoelectric dependence on size in nanoscale materials such as GaN nanowires.[91] Other studies have extended the approach to, for example, predicting alloy end member candidate compounds which might form an MPB in the composition-temperature phase space as a strategy for maximizing piezoelectric response via proximity to a phase transition.[92]

Using DFT-based tools to understand mechanistic responses of piezoelectric materials can be categorized as pertaining to the intrinsic (present in each unit cell) or extrinsic (resulting from collective interactions via domain wall motion and related phenomena) piezoelectric responses of materials.

With regard to intrinsic material properties, the material parameters most commonly computed by DFT and reported are:

(1) *Structure*. A noncentrosymmetric structure is required for piezoelectricity and should be lowest energy, or energetically accessible within the range of metastablity.
(2) *Electronic bandgap*. A wide bandgap suggests insulating character required to sustain an electric field and the possibility of low intrinsic conduction losses in piezoelectric applications.
(3) *Lattice compliance*. Dictates the strain response to the piezoelectric stress generated under applied electric field and the strain response to an applied stress which changes the polarization.
(4) *Born effective charges*. Describes the change in unit cell polarization with small displacements of atoms on a sublattice,[93] typically through the Berry-phase method.[94]
(5) *Alloying effects*. In solid-solution alloy systems, where the composition greatly influences the piezoelectric properties, understanding the changes in all of the above parameters with changes in alloy concentrations offers valuable insights into property maximization and alloy engineering.

With regard to the extrinsic piezoelectric responses, the material parameters most commonly calculated by DFT and reported are the following:

(1) *Spontaneous polarization magnitude*. In ferroelectric materials, in particular, the magnitude of the spontaneous polarization is closely tied to the potential for extrinsic contributions to the piezoelectric response.
(2) *Polymorph energies*. Energetically degenerate polymorph structures can be desired as the influence of one structure results in a modification of the observed phase with a positive effect on piezoelectric properties.[89]
(3) *Alloying energies*. The alloying effects on polymorph energies in conjunction with mixing enthalpy required for alloy formation are important for understanding the phase stability of solid-solution systems.[92]

Related to the last two points, polymorphs with similar energies to the stable structure can indicate a small energy penalty for ferroelectric domain reversal and/or in some cases, a structurally degenerate landscape which minimizes the energy penalty for piezoelectric structural deformations.[85,95,96] For this reason, inspired by knowledge of the Pb(Zr, Ti)O_3 system, high-throughput computational searches for high piezoelectric performance materials are often focused on identifying systems which could posses an MPB where the phase-energy landscape is flattened.[92,97]

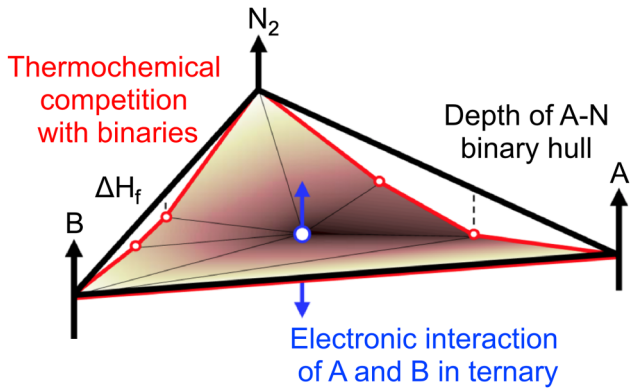

FIG. 4. Convex hull representation for ternary nitride materials showing the computed enthalpy of formation for the compound ABN_2 in relation to the binary (AN_x and BN_x) compounds. Reprinted with permission from W. Sun *et al.*, Nat. Mater. **18**, 732 (2019). Copyright 2019, Springer Nature.

C. Considerations

It is worth noting that DFT, although robust for defined boundary conditions, has limitations. First and foremost, base DFT calculations are simulated at a temperature of 0 K, and although various methods exist to estimate the effects of finite temperatures, the calculations are predominantly made to be correct at absolute zero.[98] Another consideration is that DFT methodologies are not well suited for handling the highly localized 4f electrons present in the lanthanide series.[99] This results in exclusion of lanthanides from DFT-based chemical screening studies by some groups.[85,86] Another important consideration when approaching DFT-based studies is the interpretation of formation energy and metastability, and its correlation with experimental existence of materials. When the formation energy of a material in a specific phase is compared to that of the constituent parts, known as the energy below the convex hull (see Fig. 4), it is done so to identify the lowest energy phase as a determination of what can be synthesized in the laboratory. However, the DFT-determined range of formation energies for phases which are known to be experimentally accessible can be hundreds of meV/atom above the phase predicted to be the lowest energy[100] and, even when calculated using current best practices, have typical errors around 25 meV/atom.[101] This emphasizes the importance of metastable materials, in particular, nitrides, in practical applications.

III. HIGH-THROUGHPUT SYNTHESIS AND CHARACTERIZATION OF PIEZOELECTRICS

The section which follows reviews the techniques of HTE—also known as combinatorial research—used to explore and understand piezoelectric materials. First, we discuss HTE then focus on the synthesis (Sec. III A) and characterization (Sec. III B) techniques specifically applied to piezoelectric materials. Numerous material engineering principles pertaining to piezoelectric materials originate from research of

oxide systems, and, therefore, this section includes discussion of many oxide materials.

High-throughput experimentation was first demonstrated for exploring inorganic material systems more than 50 years ago.[102,103] Since then, HTE methods have been developed and implemented at the research level for discovery and optimization of electronic, magnetic, and optical materials.[104] Reference 104 contains a brief review of HTE methodology applied to piezoelectric and ferroelectric materials, although only oxide materials are reviewed.

The basic principle of HTE is to process materials, typically in—but not limited to—thin film form, which contain a gradient in a variable of interest, such as composition. The graded material is referred to as a *library* of *samples*, where each sample has a different value for the graded variable of interest. Subsequent spatially-resolved characterization of each sample of the library allows material changes to be correlated to the graded variable. The steps involved in this methodology are illustrated graphically in Fig. 5. The parallel processing methods of HTE are significantly faster than serial processing methods traditionally employed in materials research.

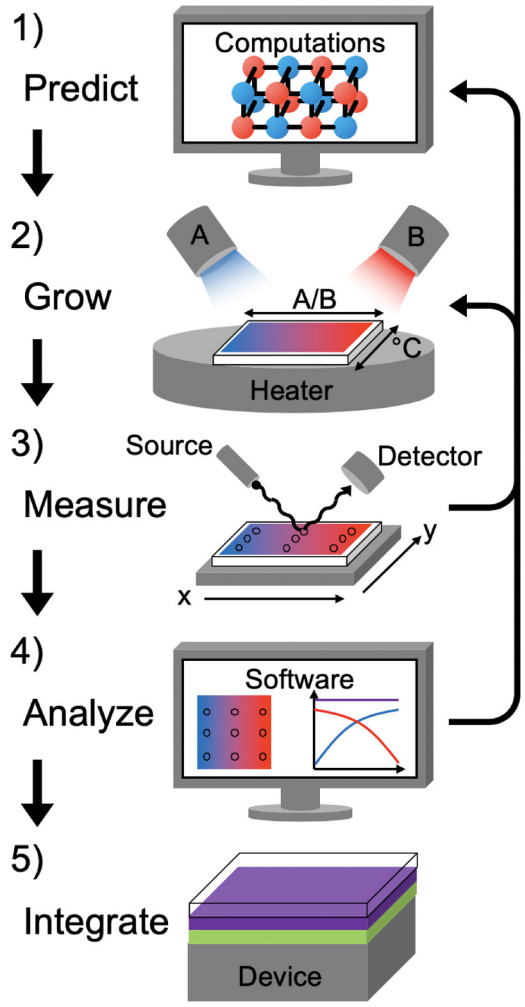

FIG. 5. Schematic depiction of a generic thin film high-throughput experimentation route: (1) Theoretical material prediction, (2) growth of a chemically-graded thin film from multiple targets, (3) characterization in a high-throughput manner to achieve large amounts of data (spectroscopic, in this case) correlated to the composition gradient, (4) analysis and processing of characterization data and correlation to combinatorial variables, and (5) integration of the material into applications. Also included are typical feedback pathways for data streams.

HTE methodology is, therefore, seen as one important tool for meeting the goals of the MGI where the time line for the materials development cycle is greatly reduced.[105] Integrated theoretical and experimental work, another hallmark of the MGI, enables deeper understanding than either can provide alone. The insights provided from high-throughput computation of materials properties and screening of chemical spaces for materials with specific attributes act to highlight areas for complementary experimental work. By pairing computation with experiments within the framework of MGI, greater progress can be made in material discovery and optimization. We focus here on historical uses of combinatorial methods in search of piezoelectric or nitride materials. Many great review articles exist which detail the specifics of combinatorial methodology and the authors suggest the following reviews for additional details:[104–108]

A. Synthesis

The basic ideas of high-throughput synthesis techniques have been adapted by a variety of research groups to meet the particular needs of their chemical systems and application requirements. A gradient in composition has frequently been the target of HTE, and common approaches to achieve such a gradient include pressing pellets with graded powder content, or more commonly, as vapor phase and liquid phase deposition onto substrates. Figure 6 shows the most common forms of combinatorial sample preparation, by vapor phase deposition and diffusion across bulk interfaces. Many mature methods for producing combinatorial samples by deposition, growth, or synthesis exist. The authors suggest the following reviews for details and applications of these methods:[105–107] The production of combinatorial libraries requires tuning the process for the simultaneous production of many materials at once, where the production of a material in a device fabrication facility optimizes the process for a single material. However, combinatorial gradients can be used to illuminate the effects of process variables on a single material. A common gradient studied in combinatorial experiments is the temperature used during the processing of the sample libraries (also shown in Fig. 6). For example, high-throughput methods have been utilized to accelerate investigation and optimization of the sintering temperature of $0.98[0.6BiFeO_3 - 0.4PbTiO_3] - 0.02Pb(Mg_{1/3}Nb_{2/3})O_3$ bulk ferroelectric ceramics.[109] Similarly, in thin films, the optimization of growth temperature in the $Sr_xBa_{1-x}Nb_2O_6$ family of ferroelectric thin films grown epitaxially by pulsed laser deposition (PLD) on a temperature-graded substrate was accomplished in a single growth run, which illustrates both the time and expense saved by HTE.[110]

In some cases, high-throughput methods are created or adapted to suit the particular needs of a characterization method where measurements are more robust for bulk

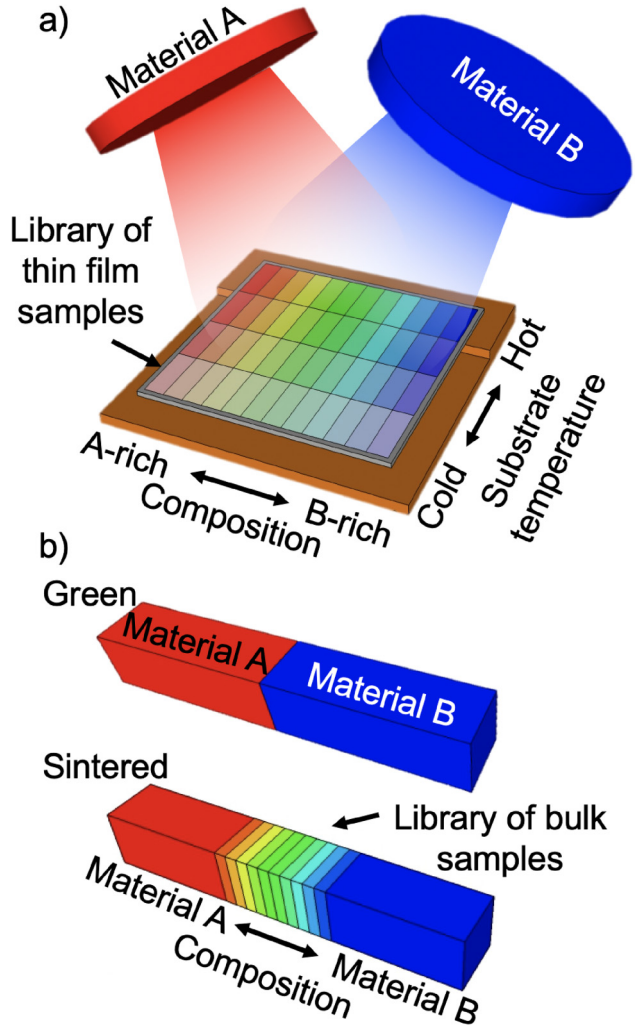

FIG. 6. Combinatorial sample synthesis schematic. (a) Thin film sample library deposited through cosputtering from two different materials which results in a compositional gradient perpendicular to a substrate temperature gradient. (b) Bulk sample library created by the heat treatment of a heterogeneous bulk interface where the diffusion of materials into each other results in a compositional gradient across the interface.

materials compared to thin films. This was the case when a high-throughput method consisting of parallel solid-state synthesis of bulk materials by mixed-oxide processing was optimized for the Pb(Zr, Ti)O_3 system, which was demonstrated to produce over 100 samples a week in a geometry compatible with their custom piezoelectric constant testing device.[111] Likewise, a method of producing inkjet printed combinatorial libraries of pellets by a robot has been demonstrated for $Ba_xSr_{1-x}TiO_3$ to eliminate some of the difficulties and artifacts associated with precisely measuring the dielectric properties of thin films.[112] In some cases, bulk methods are employed for their superior compositional control of complex systems. For example, compositionally-graded bulk ceramics have been fabricated by relying on dopant interdiffusion during sintering to create graded pellets, as was demonstrated in a study of the ferroelectric properties of $PbZr_{0.6}Ti_{0.4}O_3$ with varying levels of lanthanum and iron codoping.[113] Using a similar approach, the phase behavior of the lead-free system of $(Bi_{0.5}Na_{0.5})TiO_3 - BaTiO_3 - (K_{0.5}Na_{0.5})NbO_3$ was probed in a prime example of the high number of elements that can be incorporated in combinatorial libraries synthesized using a solid state method.[114]

Thin films are by far the most common method of creating sample libraries with composition gradients, as deposition sources can be arranged in a chamber to give rise to samples with spatially-graded compositions using many types of deposition techniques.[107] In the simplest terms, combinatorial deposition requires codeposition from spatially separated targets, so almost any chamber with more than one source can be used for combinatorial experiments. PVD techniques are particularly well suited to combinatorial synthesis because of their (primarily) line-of-sight material deposition. The majority of existing combinatorial work focuses on cation gradients from spatially separated sources, but recently methods have been demonstrated to produce gradients in the anion species as well by controllably changing the atmosphere during thin film growth, further expanding the possibilities for combinatorial thin film growth.[115] Combinatorial film growth via pulsed laser deposition (PLD) is also (relatively) straightforward and has been used, for example, for the deposition of compositionally-graded piezoelectric oxide thin films.[110]

While bulk AlN, Si_3N_4, BN, and a few other nitrides are common in bulk ceramic form, the widest variety of nitrides is most commonly fabricated by thin film techniques. Some of these techniques are less common in the field of materials discovery research, such as cathodic arc evaporation which was used to deposit libraries of metastable TiAlN films with microstructure gradients due to the incident ion energy dependence on the bias of the substrate, which was changed over the course of a deposition.[116] By far, the most popular growth technique for thin film combinatorial nitrides is reactive cosputtering from metallic targets angled toward the substrates on opposing sides in an atmosphere containing N_2 and Ar gases in which nitrides are formed by reaction with nitrogen.[89,117–121] The addition of a nitrogen plasma source, resulting in a high chemical potential for nitrogen, allows previously inaccessible metastable compounds to be realized.[119] The PVD technique has been successfully demonstrated for deposition of hard coating,[117,122–125] semiconductor,[118] and piezoelectric[66,89,121,126] nitride materials.

One of the common critiques of combinatorial syntheses such as those mentioned above is that while the chemical gradients are useful for coarse screening of chemical space, there is little control of microstructure development in resulting sample libraries. Related to this concern, combinatorial liquid source misted chemical deposition (LSMCD) can provide high-precision control of chemical composition while creating films that are more similar to materials processed in conventional serial processes; the utility of LSMCD was demonstrated via fabrication of $Bi_{3.75}La_xCe_{0.25-x}Ti_3FeO_{12}$ libraries.[127] Similarly, a robotic pipetter to deliver specifically tailored solutions of Pb(Zr, Ti)O_3 solgel precursors to spatially confined regions of a silicon wafer has been developed, producing a combinatorial library after curing.[128] These examples show the range of different methods that have been developed to achieve chemical gradients in samples optimized for different sample geometries and chemical species involved.

B. Characterization

Spatially-resolved measurement techniques are used for screening sample libraries so the measurement can be correlated to the combinatorial gradient variables, which is easier to perform in films than in the bulk form. As discussed in Sec. III A, some characterization methods are best performed on bulk material geometries not on thin films. In some instances, these are not spatially-resolved measurements, so series of bulk materials are produced with a changing variable of interest and each measured individually, as was the case for the piezoelectric measurements on Pb(Zr, Ti)O_3 ceramics.[111] In other instances, the measurement is spatially resolved, but the volume of material needed for the specific type of characterization requires bulk material geometries. This was the case for investigating the ferroelectric switching characteristics[113] and electric field-induced phase-change behavior[114] of compositionally-graded bulk ceramics where use of a combined high-energy X-ray microdiffraction and fluorescence spectroscopy setup with a coercive field applied perpendicular to the composition gradient was used. The results from this study[113] are shown in Fig. 7 as an example of the ability of this method to illuminate ferroelectric phenomena. These methods, although demonstrated successfully for bulk materials, have not been extensively adapted to thin films.

A majority of HTE characterization is performed on thin film materials because of the relative ease of gradient fabrication and the simplicity of standardizing sample handling around substrate geometry. These measurements typically involve—but are not limited to—structure and composition determination. Raman spectroscopy and x-ray diffraction provide rapid insights into crystalline structure across thin film combinatorial libraries, as demonstrated in searching for MPBs in alloy systems such as rare-earth (Sm, Gd, Dy, Nd) substituted $BiFeO_3$.[129,130] In some cases, complementary methods have been tailored for screening combinatorial libraries, such as the adaptation of cross-sectional XRD with submicrometer probe sizes, which enabled understanding of complex relationships such as links between microstructure and stress.[116] This was particularly useful given that measuring stress for combinatorial thin films is nontrivial. Researchers approached the growth-stress problem in a different way and sputtered (Al,Cr)N films directly onto cantilever arrays to more directly measure the stress during deposition and thermal processing via cantilever bowing.[125]

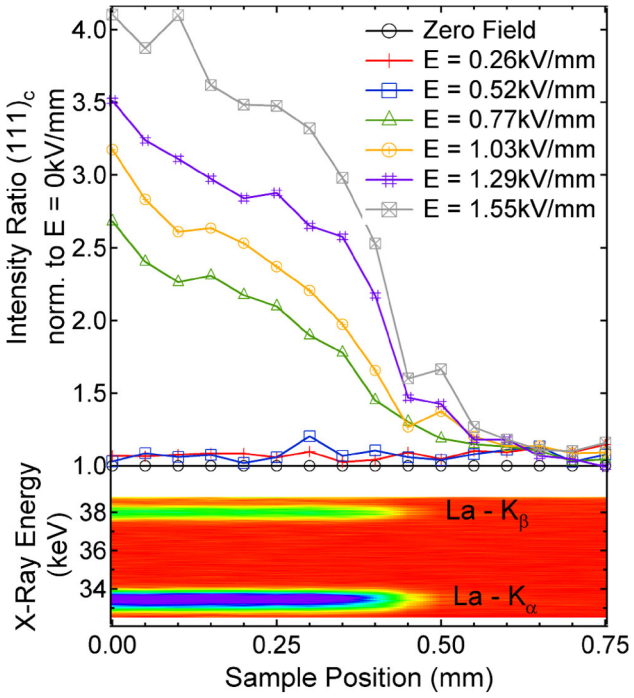

FIG. 7. Power of high-throughput combinatorial methods, utilizing bulk materials, to provide a complete picture of the effect of lanthanum dopants on switching behavior. Domain wall motion measurements for $PbZr_{0.6}Ti_{0.4}O_3$ bulk ceramics as measured by the change in intensity ratio of the diffraction peaks (top) as an electric field is applied (field strength in the legend) correlated to composition, as measured by fluorescence (bottom). Reprinted with permission from Jones *et al.*, Appl. Phys. Lett. **93**, 152904 (2008). Copyright 2008, AIP Publishing LLC.

Composition, being the most common graded variable across a sample library, is almost always measured. The most common method of combinatorial composition quantification is x-ray fluorescence (XRF) because it is relatively quick and robust without requiring significant sample preparation, but XRF suffers from poor resolution for low atomic mass elements. Therefore, a number of other techniques including electron probe microanalysis,[124] Rutherford backscattering (RBS),[119] energy-dispersive x-ray spectroscopy (EDX, EDS),[118,122] and Auger-electron spectroscopy[115] have been utilized in combinatorial studies of nitride materials, often with the purpose of quantifying oxygen impurities. Despite such techniques requiring that the measurements be carried out under vacuum, the ability to spatially resolve the results to align with individual samples on a library means that combinatorial measurements are still significantly higher-throughput than their traditional serial counterparts. Once the compositions and/or other combinatorially-graded variable(s) are quantified, other properties of interest are measured and mapped against the combinatorial gradient(s).

Nitride films have been experimentally investigated using high-throughput methods of characterization for a range of properties. $Cr_xTi_{1-x}N_y$ films were analyzed for optical properties as a function of x and y with two custom fiber-coupled CCD array spectrometers that measured in the UV-Vis and IR ranges with a programmable stage.[117] TiAlN films had a substrate bias gradient during growth to understand the effect of microstructure on mechanical properties and phase stability.[116] Transport properties of nitride semiconductors have also been investigated for materials with a tunable bandgap and electrical conductivity such as $Zn_{1-x}Sn_xN_2$,[118] $(Sn_{1-x}Ti_x)_3N_4$,[119] and $Mg_{1-x}Zr_xN_2$.[131]

Measurement techniques specific to piezoelectric materials have also been developed for high-throughput data collection. Piezoresponse force microscopy (PFM) is by far the most popular method of collecting localized data concerning piezoelectric response and, therefore, lends itself particularly well to combinatorial sample libraries.[127] However, this technique can be difficult to interpret quantitatively for

thin films because of complicating factors such as constraining substrates and competing mechanisms for producing an electromechanical response that are not piezoelectricity.[111,112,132–134] There are different approaches to this challenge. One such approach for screening piezoelectric and ferroelectric combinatorial libraries is to use a more accurately calculated figure of merit related to the d_{33} instead of the pure coefficient, which was validated for the well-known lead zirconate titanate (PZT) system.[135] One group reported direct quantitative measurements of d_{33} values for nitride piezoelectrics using a combination of PFM and scanning kelvin probe microscopy,[136] but this combination of techniques would be complicated for combinatorial libraries. In other cases, assumptions are made about the mechanical properties of the material,[121] or PFM quantification methods are not fully addressed.[130,137] In a different adaptation, the transverse piezoelectric stress coefficient ($e_{31,f}$) was determined by depositing PZT and AlN films onto Si cantilevers and performing measurements that collect charge built up while straining the cantilevers.[138] This method was complex to engineer, but extraction of meaning from the data was more straightforward than it is with PFM. This approach was not performed in a combinatorial setup, although it could be modified to do so using an array of cantilevers and a combinatorial thin film deposition technique.

Another powerful characterization method is second harmonic generation (SHG), which is specifically sensitive to broken inversion symmetry in crystals. Measurement of a second harmonic signal does not directly quantify a piezoelectric response, but because piezoelectricity requires the absence of centrosymmetry, SHG measurements can serve as sensitive complements to diffraction and other types of techniques. SHG measurements have proven useful for understanding ferroelectric hysteresis and phase transitions in bulk and thin film materials, determination of point group symmetry, measurement of nonlinear property coefficients, and—when paired with microscopic imaging—the ability to reveal domain structure.[139] These methods have been demonstrated for $KNbO_3$ thin films,[140] polycrystalline $BaTiO_3$,[141] and $BiFeO_3$ single crystals.[142]

As noted in Sec. I A, a number of other material parameters are also important for piezoelectric device design. Many of these properties are challenging to measure for thin films more directly than via extraction from prototype devices, an approach that is not generally compatible with combinatorial techniques. Recently, an iterative method described earlier[143] was adopted for accurate determination of the elastic modulus of stiff thin films on a compliant substrate using nanoindentation and applied to combinatorial samples of the (Al,Sc)N system.[144] Dielectric and ferroelectric parameters have been measured using other instruments with modification to include automated sample positioning of the probes, as was the case for combinatorial study of the $Bi_2O_3-BaO-Na_2O-TiO_2$ system.[145]

C. Considerations

Challenges associated with rapid and accurate characterization of combinatorial material libraries have inspired the development of numerous high-throughput data collection approaches. In all instances of high-throughput characterization data collection, there is a challenge to managing the large quantities of data. Analyzing these data is a nontrivial task, and, therefore, complementary to the development of high-throughput experimental tools is the development of automatic analysis algorithms[146] and data management packages,[147] which are useful aides for processing and understanding the large data sets acquired by these techniques. These packages, if adopted by the HTE community, could help to standardize the format of results for entry into open-access databases making the results more accessible and transparent to the scientific community.

As with any other measurement, repeatability of combinatorial measurements is important. Significant efforts have been invested in validating combinatorial screening tools across the community, as shown for bandgap measurements in Fig. 8. An interlaboratory collaboration between the National Renewable Energy Laboratory (NREL) and the National Institute of Standards and Technology (NIST) focused on automated collection of scanning ellipsometry, UV-vis spectroscopy, XRF, and XRD for the comparison of Zn-Sn-Ti-O combinatorial libraries grown by different thin film growth techniques from the different laboratories.[148] This study resulted in optical properties correlated to composition that were validated across synthesis and characterization techniques as seen in Fig. 8. This illustrates the power of mapping compositional space for properties of interest using the combinatorial methodology.

IV. PIEZOELECTRIC NITRIDE MATERIALS, ALN, AND BEYOND

As a relatively recent area of broad interest, the nitride piezoelectrics field has advanced rapidly in part because of simultaneous theoretical and experimental insights. We focus here on the strengths, caveats, and opportunities of such an approach. As mentioned above, many of the early studies on the piezoelectric properties of nitride semiconductors focused on mitigating the largely undesired electromechanical effects in wurtzite-based heterostructures for LEDs, quantum wells, and related devices. Examples of such are the first principles calculations of the polarization present in interfaces of III-V nitride materials used in multilayer devices[58,149] and experimental observation of the polarization effects.[150] We will not focus on this body of literature as the work was concerned with mitigating and/or compensating for piezoelectric effects rather than leveraging them, but several concepts that were matured through such efforts—particularly related to defects and heterointerfaces—are directly applicable here.

A. AlN derived alloys

The interest in nitride piezoelectrics has been fueled by the advent and growth of piezoMEMS as sensors, actuators, filters, and other related devices. Due to these successes of piezoMEMS, interest in piezoelectric AlN films increased dramatically. Numerous first principles computational studies of piezoelectric and mechanical properties, such as Ref. 151, followed, the specific results of which are highly dependent

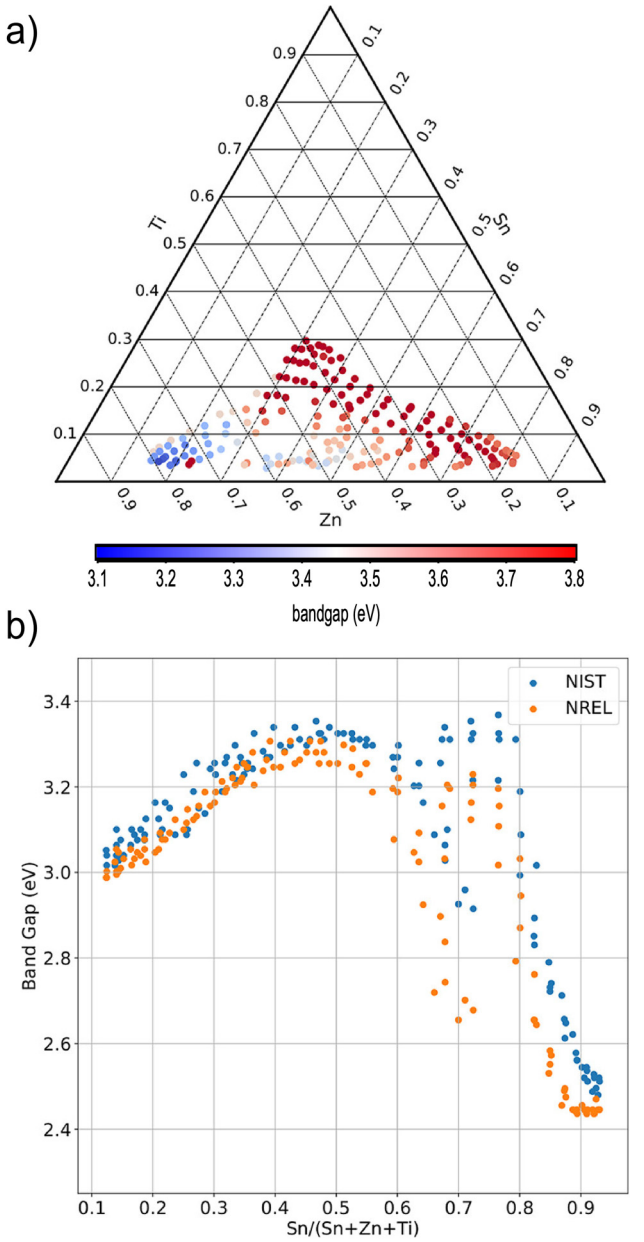

FIG. 8. Case study in the advantages of high-throughput combinatorial methods: (a) the bandgap for Zn-Sn-Ti-O libraries grown at NIST and measured by scanning ellipsometry as well as (b) a comparison to measurements performed by NREL using UV-Vis spectroscopy. Reused with permission from Hattrick-Simpers *et al.*, ACS Comb. Sci. **21**, 350 (2019). Copyright 2019, American Chemical Society.

on the exchange correlation function used within.[90] In parallel, massive experimental efforts in industrial and academic labs around the world explored the sensitivity of AlN properties to residual stress, microstructure, metallization stacks, and other variables with a focus on achieving materials with high electronic and mechanical quality.[152–157]

AlN exhibits a rather modest piezoelectric strain coefficient, so this parameter was an early target for groups looking to improve its electromechanical properties. Computation led the way in terms of early searches for non-equilibrium hexagonal nitride phases[158] and potential alloy systems with enhanced piezoelectric performance.[159] Subsequent experimental reports,[68] closely followed by excellent mechanistic discussion[160] have really focused the community's efforts on $Al_{1-x}Sc_xN$. This system is an excellent vehicle for demonstrating the importance of joint and iterative collaboration among computational and experimental materials scientists as well as device designers and process engineers. Scandium additions increase field-induced strain but also reduce the elastic stiffness of the material and introduce additional process-sensitive variables to microstructure development and residual-stress-dependence, issues that were already consuming the bandwidth of process engineers in AlN-focused fabs and foundries. Research into the complex structure-processing-property relationships in (Al, Sc)N continue in parallel (and increasingly in collaboration) with massive industry efforts to increase Sc content without sacrificing device quality or yield, all while adapting device designs to better match the modified properties of (Al,Sc)N films. While the piezoelectric material itself is the key to piezoMEMS devices, overall device performance truly is a system-level challenge in which device function depends critically on properties of all constituent materials, which vary (in some cases dramatically) with process parameters, which can vary with device design. Thus, a comprehensive understanding of the fundamental materials science of all components is crucial for efficient iterative codevelopment.

Success of $Al_{1-x}Sc_xN$ is rooted in the concept of materials metastablilty. The initial computational work on ScN and $Sc_{1-x}Ga_xN$, which inspired $Al_{1-x}Sc_xN$, proposed material systems which were predicted to be metastable.[158] As discussed in Ref. 89, the $Al_{1-x}Sc_xN$ alloy system is thermodynamically unstable (Fig. 9). It can nevertheless be successfully realized and exploited because of the energetic deposition processes involved, but this inherent instability leads to difficulties in achieving high quality materials at high alloying levels. However, related to metastability, a recent report of ferroelectric polarization switching combined with tunability of the coercive field through alloy composition in the $Al_{1-x}Sc_xN$ system[161] is bound to further increase the amount of work within this materials space and add another layer of complexity to both optimization of these materials and continued exploration for new piezoelectrics.

Nitride materials naturally lend themselves to the formation of thermodynamically unstable phases, due to large formation energy of N_2 molecules,[52] as well as large cohesive energy leading to hindered kinetics, ultimately allowing for a higher tolerance of metastability compared to other anion systems.[100] Additionally, the larger window of metastability in heterostructural alloys due to the energy barrier of reconstructive phase transformations (compared to isostructural alloys) can lead to formation of materials even deeper within metastable phase space. Figure 9 illustrates this as well; metastable regions are accessible at plasma energies, and can be retained at lower temperatures because of limited kinetic pathways for reconstructive decomposition. For these reasons, theoretical work in this field is commonly interested in leveraging metastability for designing new piezoelectric material systems, free from the constraints of a thermodynamic ground state.

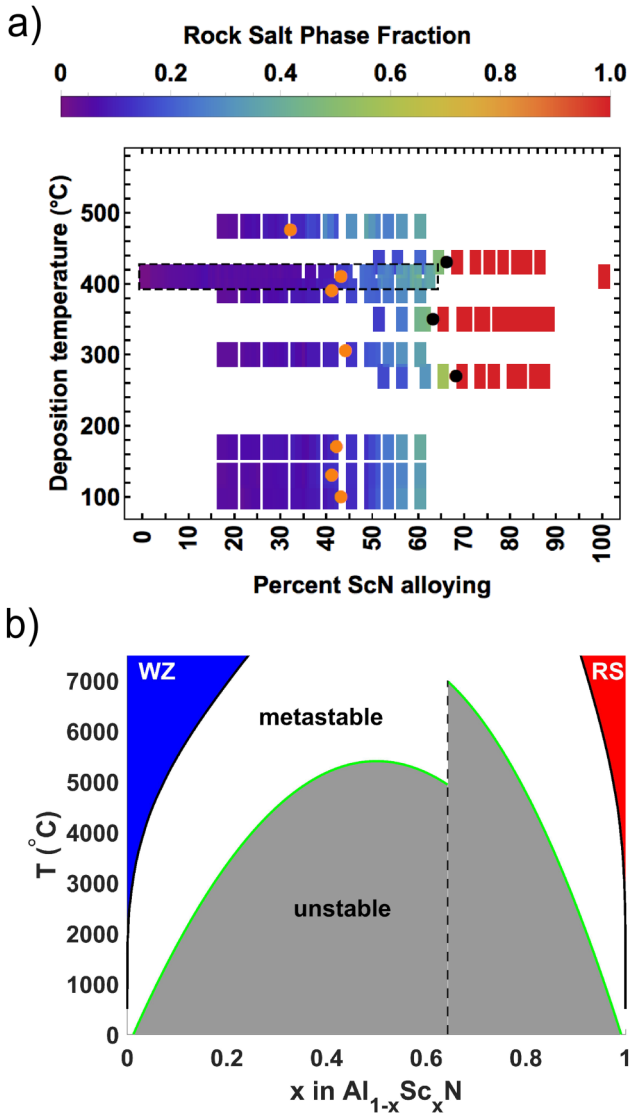

FIG. 9. Temperature-composition phase space of the $Al_{1-x}Sc_xN$ system (a) determined by reactive sputtering and structural analysis and (b) predicted computationally. The difference in observed mixed phase regions [between orange and black markers in (a) and inside unstable region in (b)] indicate a high level of metastability at work within this system. Reproduced and modified from Talley *et al.*, Phys. Rev. Mater. **2**, 63802 (2018). Copyright 2018 Authors, under a Creative Commons Attribution 4.0 International License.

Much of the subsequent computational efforts directed toward discovery and development of new piezoelectric nitride materials fall into one of the following three categories. Certainly each of these approaches has its own strengths and limitations, and many groups—including our own—have had success with each.

1. Explore fundamental underpinnings of the AlN and/or $Al_{1-x}Sc_xN$ systems with the goal of furthering mechanistic understanding to educate new alloy choices.[89,162]
2. Replace Sc (or, more directly, Al) with another trivalent (or trivalent-equivalent) cation(s) and directly calculate properties as a function of alloy composition.[120,163,164]
3. Identify non-AlN (and often nonwurtzite) nitrides that appear to be energetically stable (or at least accessible) and have promising piezoelectric properties.[84,86,165]

The greatest gains tend to arise from studies that combine multiple approaches and/or couple computation with experiment to understand existing materials or identify new alloy systems. Examples include paired computation and high-throughput experiment for understanding the metastability and miscibility gaps in AlN based alloy systems $Al_{1-x}Sc_xN$,[89] $Al_{1-x}Cr_xN$,[120] and $Al_{1-x}Ti_xN$.[162] The experimental portions of these studies all used combinatorial sputtered thin films to efficiently explore the composition dependence of microstructure and phase stability along with DFT-based computation to help explain and interpret the results of experiments. In some cases, the predictions provided by DFT were also investigated experimentally using HTE, such as the case for $Al_{1-x}(Mg/Hf)_xN$.[121] These sample libraries were analyzed for phase evolution and heterostructural alloy solubility as a function of chemical composition and, in one case (Ref. 89), a thermal gradient during film deposition.[89,120,121] However, experimental piezoelectric properties for these films were only reported in one paper, and it was investigated using PFM.[121] Codoping schemes for AlN alloys, proposed and evaluated with DFT modeling[163] relaxes the need for trivalent dopants and suggest piezoelectric performance can be improved when two aluminum cations are substituted with a 4^+ and 2^+ cation pair such as Mg–Hf or Mg–Zr. This approach also suggested using doping schemes where the average cation size is comparable to aluminum for improved lattice stability.

B. Materials beyond AlN

The search for new piezoelectric materials in nitride space has journeyed beyond the AlN system, primarily following piezoelectric design principles developed through decades of work on oxide piezoelectrics. The highest-performance oxide piezoelectrics all exhibit a perovskite structure, so searching for perovskites was a natural place to start. Recent reports have identified potentially stable nitride perovskite materials in such studies;[84,86] the results of one such chemical screening are shown in Fig. 10. This study found 21 new ABN_3 compositions, 3 of which were predicted as perovskites, one being $LaWN_3$.[86] Another study of similar focus, highlighted in Fig. 3, found 71 new ABX_3 perovskites, including 12 with promising piezoelectric and ferroelectric character, one also being $LaWN_3$.[84]

In both of these studies $LaWN_3$ was identified as a stable perovskite suitable for piezoelectric applications. In fact, the material showed enough promise that others followed with higher accuracy calculations of the predicted piezoelectric and even ferroelectric properties.[165] Such predictions still await experimental confirmation. Recent reports of oxygen-substituted $LaWO_{0.5}N_{2.5}$ demonstrate interest in this material, but more importantly the difficulty of processing pure nitride materials that contain highly oxyphilic elements.[166]

Breaking away from typical piezoelectric design principles has identified additional materials worth exploring. One

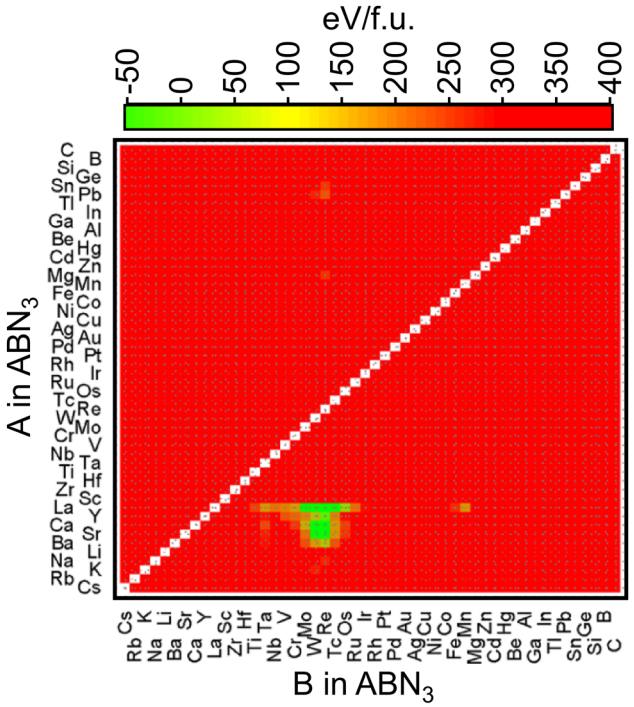

FIG. 10. DFT determined formation energy, relative to the convex hull, for nitride perovskites across a majority of the periodic table, but excluding lanthanides greater than lanthanum. Reprinted with permission from R. Sarmiento-Pérez, T. F. T. Cerqueira, S. Körbel, S. Botti, and M. A. L. Marques, Chem. Mater. **27**, 5957 (2015). Copyright 2015, American Chemical Society.

such approach is to find materials that exhibit a quasi-2D layer structure, defined as bulk 3D crystals in which bonding in one direction is dominated by soft van der Waals bonds along at least one direction. A recent computational screening study identified 51 such candidates, including nitride materials (e.g., NaSnN) with calculated piezoelectric strain coefficients each greater than 30 pC/N.[167] The possibilities awaiting the piezoelectric community extend beyond the oxide and nitride material families, though there are certainly options left to explore even within that space. For example, while ferroelectricity is certainly not required for piezoelectric response, it is found in many of the highest-performance piezoelectric materials (including $Al_{1-x}Sc_xN$[161]) and may open up even more device architectures. There are reports of ferroelectric switching in $CuInP_2S_6$ flakes of only 4 nm thickness, being essentially two dimensional in form[168] and ferroelectricity has been predicted in GaS, GaSe, SnS, and SnSe monolayered materials.[169] For more information on the topic of 2D piezoelectric materials, the authors suggest a recent review on this subject, Ref. 170.

V. STATE OF THE FIELD AND DIRECTIONS FOR CONTINUED WORK

Nitride combinatorial studies have thus far only been reported using thin film deposition techniques. The films have been studied for high-hardness,[117] semiconductor,[118,119] and piezoelectric applications,[89,120,121] although this represents only a handful of the fields in which nitrides are used. The search for materials with greatly improved performance over $Al_{1-x}Sc_xN$ is still in the very early stages, but increased attention is being directed toward this material space via a number of different approaches. The tightly coupled application of computational and experimental approaches shows great promise for efficiently exploring and understanding piezoelectric nitride materials and beyond. The studies which seem to be the most insightful are those which leverage underlying mechanistic principles from known piezoelectric systems in order to target new material families without simply chasing first-order similarities. A recent report of ferroelectric polarization switching combined with tunability of the coercive field through alloy composition in the $Al_{1-x}Sc_xN$ system[161] is bound to further increase the amount of work within this materials space and add another layer of complexity to both optimization of these materials and continued exploration for new piezoelectrics.

The theoretical community continues to provide significant insights into the underpinnings of known piezoelectric nitride systems that help to both target and realize improved material quality and performance. In turn, the information gained from high-throughput experimental work rapidly feeds back to theoretical and computational efforts to iteratively improve mechanistic descriptions and predictions. This continued blurring of the walls among theory, computation, experiment, and device design is crucial to efficient exploration and exploitation of new materials, and nitride piezoelectrics exemplify this as well as any material family.

High-throughput experimental exploration of piezoelectric nitride materials has matured significantly but continues to expand. The addition of machine learning to the field of materials discovery will offer new avenues of exploration.[171–173] Chemical gradients are the default variable across combinatorial libraries, but thermal, stress, and substrate bias gradients have also been the subject of investigations. Future areas that could be explored via combinatorial libraries include gradients in the surface functionalization, gradients in athermal processing energies (e.g., chemical potential, pressure, voltage, optical, others), or combined gradients in chemical compositions and processing parameters. Utilizing some of the methods benchmarked for high-throughput exploration of oxide piezoelectric materials in the nitride families will further inform a deeper understanding of these systems.

Parallelized measurement and characterization tools as well as associated data handling tools are gradually converging on a small number of *de facto* standards, facilitating data sharing and reuse. The techniques frequently involve automated sample positioning, which is key for reducing human input hours. While many needs (such as chemical identification, phase identification, etc.) are met by the developing set of characterization tools, microstructure analysis by electron microscopy remains largely serial and labor intensive in most combinatorial laboratories. Some groups have developed appropriate workflows for accelerating this process but implementation remains limited. While additional tools are certain to arise as more high-throughput characterization and synthesis methods emerge, continued and expanded interoperability becomes even more crucial for expanded data sharing and reuse via modern data tools.[82,147]

The piezoelectric properties of combinatorial film libraries have only been probed (and reported) with PFM, which has the advantage of providing localized data on a scannable platform,[121] but the flexibility and sensitivity of the technique make it susceptible to convolution of a number of factors, greatly complicating reliable quantitative extraction of pure piezoelectric response.[132–134] Greater adoption of complementary techniques such as double beam laser interferometry[174–176] in a combinatorial fashion is encouraged, but will likely require advances that simplify optical alignment and reduce initial cost.

The quest to identify and improve piezoelectric nitride materials continues in several directions. $Al_{1-x}Sc_xN$ is well-positioned to dominate both legacy and many emerging piezoMEMS applications in the near future. As design and integration tool flexibility continue to improve, there are significant opportunities for new compositions with extended functionality. A number of promising proposed modifications to AlN remain to be experimentally validated, and more will certainly emerge as theory and models continue to improve while strategies for modification expand and change. Beyond AlN-based systems, the proposed systems of $LaWN_3$ and NaSnN need experimental verification, and mixed anion systems remain largely unexplored. In short, we are in an exciting time where theoretical understanding, computational and simulation tools, fabrication control, and measurement/characterization tools are all converging to provide near-atomic fidelity in a sufficiently rapid, iterative, and in some cases nearly-autonomous manner to dramatically accelerate the material discovery, development, and deployment process.

ACKNOWLEDGMENTS

K.R.T. and G.B. acknowledge support by the United States National Science Foundation (NSF) Award (No. DMREF-1534503). R.S. has been supported by a CoorsTek Fellowship in Advanced Ceramics and the National Science Foundation Graduate Research Fellowship Program under Grant No. 1646713. A.Z. acknowledges funding by the U.S. Department of Energy (DOE), Office of Science, Office of Basic Energy Sciences, under Contract No. DE-AC36-08GO28308 to National Renewable Energy Laboratory (NREL). Any opinions, findings, conclusions, or recommendations expressed within are those of the authors and do not reflect the views of the National Science Foundation, Colorado School of Mines, the U.S. Department of Energy, or the U.S. Government.

[1]J. Curie and P. Curie, Bull. Minér. **3**, 90 (1880).
[2]P. K. Panda and B. Sahoo, Ferroelectrics **474**, 128 (2015).
[3]M. Krames *et al.*, Phys. Status Solidi (a) **192**, 237 (2002).
[4]S. Vepřek and S. Reiprich, Thin Solid Films **268**, 64 (1995).
[5]J. Zhu, P. Xiao, H. Li, and S. A. Carabineiro, ACS Appl. Mater. Interfaces **6**, 16449 (2014).
[6]D. Damjanovic and R. E. Newnham, J. Intell. Mater. Syst. Struct. **3**, 190 (1992).
[7]C. R. Bowen, H. A. Kim, P. M. Weaver, and S. Dunn, Energy Environ. Sci. **7**, 25 (2014).
[8]S. Trolier-Mckinstry and P. Muralt, J. Electroceram. **12**, 7 (2004).
[9]C. Fei, X. Liu, B. Zhu, D. Li, X. Yang, Y. Yang, and Q. Zhou, Nano Energy **51**, 146 (2018).
[10]J. DeKlerk and E. F. Kelly, Rev. Sci. Instrum. **36**, 506 (1965).
[11]Y. Q. Fu *et al.*, Prog. Mater. Sci. **89**, 31 (2017).
[12]S. Tadigadapa and K. Mateti, Meas. Sci. Technol. **20**, 092001 (2009).
[13]L. Qin and Q.-M. Wang, J. Appl. Phys. **107**, 114102 (2010).
[14]L. Qin and Q.-M. Wang, J. Appl. Phys. **108**, 104510 (2010).
[15]H. Joffe, D. Berlincourt, H. Krueger, and L. Shiozawa, *14th Annual Symposium on Frequency Control, Atlantic City, NJ, 31 May–2 June 1960* (IEEE, Piscataway, NJ, 1960), Vol. 19.
[16]K. F. Young and H. P. R. Frederikse, J. Phys. Chem. Ref. Data **2**, 313 (1973).
[17]J. Tichỳ, J. Erhart, E. Kittinger, and J. Privratska, *Fundamentals of Piezoelectric Sensorics: Mechanical, Dielectric, and Thermodynamical Properties of Piezoelectric Materials* (Springer, Berlin, 2010).
[18]T. Kamiya, Jpn. J. Appl. Phys. **35**, 4421 (1996).
[19]I. L. Guy, S. Muensit, and E. M. Goldys, Appl. Phys. Lett. **75**, 4133 (1999).
[20]D. F. Crisler, J. J. Cupal, and A. R. Moore, Proc. IEEE **56**, 225 (1968).
[21]S. Muensit, E. M. Goldys, and I. L. Guy, Appl. Phys. Lett. **75**, 3965 (1999).
[22]C.-Y. Nam, P. Jaroenapibal, D. Tham, D. E. Luzzi, S. Evoy, and J. E. Fischer, Nano Lett. **6**, 153 (2006).
[23]P. Gao *et al.*, Microscopy **59**, 285 (2010).
[24]R. Turner, P. Fuierer, R. Newnham, and T. Shrout, Appl. Acoust. **41**, 299 (1994).
[25]C. R. Hill, J. C. Bamber, and G. R. Ter Haar, *Physical Principles of Medical Ultrasonics* (Wiley, New York, 2005).
[26]W. S. Yan, R. Zhang, Z. L. Xie, X. Q. Xiu, Y. D. Zheng, Z. G. Liu, S. Xu, and Z. H. He, Appl. Phys. Lett. **94**, 242111 (2009).
[27]V. Fuflyigin, E. Salley, A. Osinsky, and P. Norris, Appl. Phys. Lett. **77**, 3075 (2000).
[28]S. B. Lang, Phys. Today **58**, 31 (2005).
[29]C. Wood and D. Jena, *Polarization Effects in Semiconductors: From Ab Initio Theory to Device Applications* (Springer, Berlin, 2007).
[30]S. A. Wilson *et al.*, Mater. Sci. Eng. R Rep. **56**, 1 (2007).
[31]W. Utsumi, H. Saitoh, H. Kaneko, T. Watanuki, K. Aoki, and O. Shimomura, Nat. Mater. **2**, 735 (2003).
[32]V. Kudyakova, R. Shishkin, A. Elagin, M. Baranov, and A. Beketov, J. Eur. Ceram. Soc. **37**, 1143 (2017).
[33]D. W. Lane, K. D. Rogers, J. D. Painter, D. A. Wood, and M. E. Ozsan, Thin Solid Films **361**, 1 (2000).
[34]L. Bayarjargal and B. Winkler, Appl. Phys. Lett. **100**, 021909 (2012).
[35]D. R. Spearing, I. Farnan, and J. F. Stebbins, Phys. Chem. Miner. **19**, 307 (1992).
[36]G. Hayward, J. Bennett, and R. Hamilton, J. Acoust. Soc. Am. **98**, 2187 (1995).
[37]R. Zhang, B. Jiang, and W. Cao, J. Appl. Phys. **90**, 3471 (2001).
[38]R. S. Weis and T. K. Gaylord, Appl. Phys. A **37**, 191 (1985).
[39]K. C. Cheng, H. L. W. Chan, C. L. Choy, Q. Yin, H. Luo, and Z. Yin, IEEE Trans. Ultrason. Ferroelectr. Freq. Control **50**, 1177 (2003).
[40]G. Ohlendorf, D. Richter, J. Sauerwald, and H. Fritze, Diff. Fundam. **8**, 6 (2008).
[41]K.-S. Hong, H. Xu, H. Konishi, and X. Li, J. Phys. Chem. Lett. **1**, 997 (2010).
[42]D. Berlincourt, H. Krueger, and C. Near, Technical publication TP-226, 2003, see www.morgan-electroceramics.com.
[43]G. Sebald, E. Lefeuvre, and D. Guyomar, IEEE Trans. Ultrason. Ferroelectr. Freq. Control **55**, 538 (2008).
[44]B. Jaffe, *Piezoelectric Ceramics* (Elsevier, New York, 2012), Vol. 3.
[45]Y.-H. Chen, K. Uchino, M. Shen, and D. Viehland, J. Appl. Phys. **90**, 1455 (2001).
[46]R. E. Newnham, *Properties of Materials: Anisotropy, Symmetry, Structure* (Oxford University, Oxford, 2005).
[47]IUCr, *International Tables for Crystallography, Volume A: Space Group Symmetry*. International Tables for Crystallography (Kluwer Academic, Dordrecht), Vol. 5, revised edition, 2002.
[48]S. Gevorgian, A. K. Tagantsev, and A. Vorobiev, "Dielectric, mechanical, and electromechanical properties of ferroelectrics and piezoelectrics," in *Tuneable Film Bulk Acoustic Wave Resonators* (Springer, Berlin, 2013), Chap. 2, pp. 17–54.
[49]J. Nye and P. Nye, *Physical Properties of Crystals: Their Representation by Tensors and Matrices* (Clarendon, Oxford, 1985).
[50]S. Zhang, R. Xia, L. Lebrun, D. Anderson, and T. R. Shrout, Mater. Lett. **59**, 3471 (2005).

[51]F. J. DiSalvo and S. J. Clarke, ChemInform **27**, 241 (2010).
[52]A. Zakutayev, J. Mater. Chem. A **4**, 6742 (2016).
[53]W. Sun *et al.*, Nat. Mater. **18**, 732 (2019).
[54]S. Clarke, "Nitrides," in *Encyclopedia of Materials: Science and Technology*, edited by K. J. Buschow, R. W. Cahn, M. C. Flemings, B. Ilschner, E. J. Kramer, S. Mahajan, and P. Veyssière (Elsevier, Oxford, 2001), pp. 6161–6163.
[55]M. Takahashi, G.-C. Lai, K. Ohta, and F. Kanamaru, "Bond strength and thermal stability of transition metal nitrides," in *Advances in Quantum Chemistry* (Academic, New York, 1998), Vol. 29, pp. 253–268.
[56]I. M. Watson, Coord. Chem. Rev. **257**, 2120 (2013).
[57]B. Monemar, J. Mater. Sci. Mater. Electron. **10**, 227 (1999).
[58]J. S. Speck and S. F. Chichibu, MRS Bull. **34**, 304 (2011).
[59]D. Jena *et al.*, Jpn. J. Appl. Phys. **58**, SC0801 (2019).
[60]F. Bernardini and V. Fiorentini, Appl. Surf. Sci. **166**, 23 (2000).
[61]E. T. Yu, X. Z. Dang, P. M. Asbeck, S. S. Lau, and G. J. Sullivan, J. Vac. Sci. Technol. B **17**, 1742 (2002).
[62]R. A. Beach and T. C. McGill, J. Vac. Sci. Technol. B **17**, 1753 (2002).
[63]A. Ababneh, M. Alsumady, H. Seidel, T. Manzaneque, J. Hernando-García, J. Sánchez-Rojas, A. Bittner, and U. Schmid, Appl. Surf. Sci. **259**, 59 (2012).
[64]*Aluminum Nitride (AlN) Piezoelectric Constants, Electromechanical Coupling Factor*, edited by O. Madelung, U. Rössler, and M. Schulz (Springer, Berlin, 2001), pp. 1–4.
[65]M. A. Dubois and P. Muralt, Appl. Phys. Lett. **74**, 3032 (1999).
[66]M. A. Dubois and P. Muralt, J. Appl. Phys. **89**, 6389 (2001).
[67]G. F. Iriarte, J. G. Rodríguez, and F. Calle, Mater. Res. Bull. **45**, 1039 (2010).
[68]M. Akiyama, K. Kano, and A. Teshigahara, Appl. Phys. Lett. **95**, 162107 (2009).
[69]P. Hohenberg and W. Kohn, Phys. Rev. **136**, 864 (1964).
[70]W. Kohn, A. D. Becke, and R. G. Parr, J. Phys. Chem. **100**, 12974 (1996).
[71]P. J. Hasnip, K. Refson, M. I. Probert, J. R. Yates, S. J. Clark, and C. J. Pickard, Philos. Trans. R. Soc. A Math. Phys. Eng. Sci. **372**, 20130270 (2014).
[72]W. Kohn and L. J. Sham, Phys. Rev. **140**, 1133 (1965).
[73]J. P. Perdew, K. Burke, and M. Ernzerhof, Phys. Rev. Lett. **77**, 3865 (1996).
[74]V. I. Anisimov, F. Aryasetiawan, and A. I. Lichtenstein, J. Phys. Condens. Matter **9**, 767 (1997).
[75]G. Kresse and J. Furthmüller, Phys. Rev. B **54**, 11169 (1996).
[76]A. Zunger, S.-H. Wei, L. G. Ferreira, and J. E. Bernard, Phys. Rev. Lett. **65**, 353 (1990).
[77]H. Peng and S. Lany, Phys. Rev. B **87**, 174113 (2013).
[78]A. Jain, K. A. Persson, and G. Ceder, APL Mater. **4**, 053102 (2016).
[79]C. E. Calderon *et al.*, Comput. Mater. Sci. **108**, 233 (2015).
[80]A. Jain *et al.*, APL Mater. **1**, 011002 (2013).
[81]M. De Jong, W. Chen, H. Geerlings, M. Asta, and K. A. Persson, Sci. Data **2**, 150053 (2015).
[82]A. Zakutayev, N. Wunder, M. Schwarting, J. D. Perkins, R. White, K. Munch, W. Tumas, and C. Phillips, Sci. Data **5**, 180053 (2018).
[83]Y. Xu, M. Yamazaki, and P. Villars, Jpn. J. Appl. Phys. **50**, 11RH02 (2011).
[84]S. Körbel, M. A. L. Marques, and S. Botti, J. Mater. Chem. C **4**, 3157 (2016).
[85]R. Armiento, B. Kozinsky, M. Fornari, and G. Ceder, Phys. Rev. B **84**, 14103 (2011).
[86]R. Sarmiento-Pérez, T. F. T. Cerqueira, S. Körbel, S. Botti, and M. A. L. Marques, Chem. Mater. **27**, 5957 (2015).
[87]A. Roy, J. W. Bennett, K. M. Rabe, and D. Vanderbilt, Phys. Rev. Lett. **109**, 037602 (2012).
[88]C. Tholander, F. Tasnádi, I. A. Abrikosov, L. Hultman, J. Birch, and B. Alling, Phys. Rev. B **92**, 174119 (2015).
[89]K. R. Talley, S. L. Millican, J. Mangum, S. Siol, C. B. Musgrave, B. Gorman, A. M. Holder, A. Zakutayev, and G. L. Brennecka, Phys. Rev. Mater. **2**, 063802 (2018).
[90]F. Bernardini and V. Fiorentini, Appl. Phys. Lett. **80**, 4145 (2002).
[91]R. Agrawal and H. D. Espinosa, Nano Lett. **11**, 786 (2011).
[92]R. Armiento, B. Kozinsky, G. Hautier, M. Fornari, and G. Ceder, Phys. Rev. B **89**, 134103 (2014).
[93]X. Gonze and C. Lee, Phys. Rev. B **55**, 10355 (1997).
[94]M. V. Berry, Proc. R. Soc. Lond. A Math. Phys. Sci. **392**, 45 (1984).
[95]P. Ghosez, E. Cockayne, U. V. Waghmare, and K. M. Rabe, Phys. Rev. B **60**, 836 (1999).
[96]S. V. Halilov, M. Fornari, and D. J. Singh, Appl. Phys. Lett. **81**, 3443 (2002).
[97]H. Liu, J. Chen, H. Huang, L. Fan, Y. Ren, Z. Pan, J. Deng, L. Q. Chen, and X. Xing, Phys. Rev. Lett. **120**, 055501 (2018).
[98]D. S. Sholl and J. A. Steckel, "DFT calculations of vibrational frequencies," in *Density Functional Theory* (Wiley, Hoboken, NJ, 2009), Chap. 5, Vol. 113.
[99]J. B. Morée and B. Amadon, Phys. Rev. B **98**, 205101 (2018).
[100]W. Sun, S. T. Dacek, S. P. Ong, G. Hautier, A. Jain, W. D. Richards, A. C. Gamst, K. A. Persson, and G. Ceder, Sci. Adv. **2**, e1600225 (2016).
[101]G. Hautier, S. Ping Ong, A. Jain, C. J. Moore, and G. Ceder, Phys. Rev. B **85**, 155208 (2012).
[102]A. Boettcher, G. Haase, and R. Thun, Z. Metallkd. **46**, 386 (1955).
[103]K. Kennedy, T. Stefansky, G. Davy, V. F. Zackay, and E. R. Parker, J. Appl. Phys. **36**, 3808 (1965).
[104]M. L. Green, I. Takeuchi, and J. R. Hattrick-Simpers, J. Appl. Phys. **113**, 231101 (2013).
[105]M. L. Green *et al.*, Appl. Phys. Rev. **4**, 11105 (2017).
[106]W. F. Maier, K. Stowe, and S. Sieg, Angew. Chem. **46**, 6016 (2007).
[107]P. J. McGinn, ACS Comb. Sci. **21**, 501 (2019).
[108]R. Potyrailo, K. Rajan, K. Stoewe, I. Takeuchi, B. Chisholm, and H. Lam, ACS Comb. Sci. **13**, 579 (2011).
[109]W. Hu, X. Tan, and K. Rajan, Appl. Phys. A Mater. Sci. Process. **99**, 427 (2010).
[110]I. Ohkubo, H. M. Christen, S. V. Kalinin, G. E. Jellison, C. M. Rouleau, and D. H. Lowndes, Appl. Phys. Lett. **84**, 1350 (2004).
[111]A. Cardin, B. Wessler, C. Schuh, T. Steinkopff, and W. F. Maier, J. Electroceram. **19**, 267 (2007).
[112]R. C. Pullar *et al.*, J. Eur. Ceram. Soc. **27**, 4437 (2007).
[113]J. L. Jones, A. Pramanick, and J. E. Daniels, Appl. Phys. Lett. **93**, 152904 (2008).
[114]J. E. Daniels, W. Jo, J. Rödel, V. Honkimäki, and J. L. Jones, Acta Mater. **58**, 2103 (2010).
[115]Y. Han, B. Matthews, D. Roberts, K. R. Talley, S. R. Bauers, C. Perkins, Q. Zhang, and A. Zakutayev, ACS Comb. Sci. **20**, 436 (2018).
[116]A. Riedl *et al.*, Surf. Coat. Technol. **257**, 108 (2014).
[117]C. W. Teplin, Appl. Surf. Sci. **223**, 253 (2004).
[118]A. N. Fioretti, A. Zakutayev, H. Moutinho, C. Melamed, J. D. Perkins, A. G. Norman, M. Al-Jassim, E. S. Toberer, and A. C. Tamboli, J. Mater. Chem. C **3**, 11017 (2015).
[119]A. Bikowski, S. Siol, J. Gu, A. Holder, J. S. Mangum, B. Gorman, W. Tumas, S. Lany, and A. Zakutayev, Chem. Mater. **29**, 6511 (2017).
[120]S. Manna, K. R. Talley, P. Gorai, J. Mangum, A. Zakutayev, G. L. Brennecka, V. Stevanović, and C. V. Ciobanu, Phys. Rev. Appl. **9**, 034026 (2018).
[121]H. H. Nguyen, H. Oguchi, L. Van Minh, and H. Kuwano, ACS Comb. Sci. **19**, 365 (2017).
[122]T. Reeswinkel, D. G. Sangiovanni, V. Chirita, L. Hultman, and J. M. Schneider, Surf. Coat. Technol. **205**, 4821 (2011).
[123]B. Krause, S. Darma, M. Kaufholz, S. Mangold, S. Doyle, S. Ulrich, H. Leiste, M. Stüber, and T. Baumbach, J. Appl. Crystallogr. **46**, 1064 (2013).
[124]S. Spitz, M. Stueber, H. Leiste, S. Ulrich, and H. J. Seifert, Surf. Coat. Technol. **237**, 149 (2013).
[125]D. Grochla, A. Siegel, S. Hamann, P. J. Buenconsejo, M. Kieschnick, H. Brunken, D. König, and A. Ludwig, J. Phys. D Appl. Phys. **46**, 084011 (2013).
[126]T. Yokoyama, Y. Iwazaki, Y. Onda, Y. Sasajima, T. Nishihara, and M. Ueda, *2014 IEEE International Ultrasonics Symposium*, Chicago, IL, 3–6 September 2014 (IEEE, Piscataway, NJ, 2014).
[127]K. W. Kim, M. K. Jeon, K. S. Oh, T. S. Kim, Y. S. Kim, and S. I. Woo, Proc. Natl. Acad. Sci. U.S.A. **104**, 1134 (2007).
[128]D. Rende, K. Schwarz, U. Rabe, W. F. Maier, and W. Arnold, Prog. Solid State Chem. **35**, 361 (2007).
[129]D. Kan, C. J. Long, C. Steinmetz, S. E. Lofland, and I. Takeuchi, J. Mater. Res. **27**, 2691 (2012).
[130]M. S. Darby, D. V. Karpinsky, J. Pokorny, S. Guerin, A. L. Kholkin, S. Miao, B. E. Hayden, and I. M. Reaney, Thin Solid Films **531**, 56 (2013).
[131]S. R. Bauers, D. M. Hamann, A. Patterson, J. D. Perkins, K. R. Talley, and A. Zakutayev, Jpn. J. Appl. Phys. **58**, SC1015 (2019).
[132]D. Seol, B. Kim, and Y. Kim, Curr. Appl. Phys. **17**, 661 (2017).

[133]A. N. Morozovska, E. A. Eliseev, S. L. Bravina, and S. V. Kalinin, Phys. Rev. B **75**, 1 (2007).
[134]S. V. Kalinin, A. Rar, and S. Jesse, IEEE Trans. Ultrason. Ferroelectr. Freq. Control **53**, 2226 (2006).
[135]R. P. Herber, C. Schröter, B. Wessler, and G. A. Schneider, Thin Solid Films **516**, 8609 (2008).
[136]B. J. Rodriguez, A. Gruverman, A. I. Kingon, and R. J. Nemanich, J. Cryst. Growth **246**, 252 (2002).
[137]T. Takeuchi *et al.*, Appl. Phys. Lett. **73**, 1691 (1998).
[138]M. A. Dubois and P. Muralt, Sens. Actuators A Phys. **77**, 106 (1999).
[139]S. A. Denev, T. T. Lummen, E. Barnes, A. Kumar, and V. Gopalan, J. Am. Ceram. Soc. **94**, 2699 (2011).
[140]V. Gopalan and R. Raj, Appl. Phys. Lett. **68**, 1323 (1995).
[141]M. H. Frey and D. A. Payne, Phys. Rev. B **54**, 3158 (1996).
[142]H. Yokota, R. Haumont, J. M. Kiat, H. Matsuura, and Y. Uesu, Appl. Phys. Lett. **95**, 082904 (2009).
[143]H. Li and J. J. Vlassak, J. Mater. Res. **24**, 1114 (2009).
[144]D. Wu, Y. Chen, S. Manna, K. Talley, A. Zakutayev, G. L. Brennecka, C. V. Ciobanu, P. Constantine, and C. E. Packard, IEEE Trans. Ultrason. Ferroelectr. Freq. Control **65**, 2167 (2018).
[145]B. E. Hayden and S. Yakovlev, Thin Solid Films **603**, 108 (2016).
[146]J. R. Hattrick-Simpers, J. M. Gregoire, and A. G. Kusne, APL Mater. **4**, 53211 (2016).
[147]K. R. Talley *et al.*, ACS Comb. Sci. **21**, 537 (2019).
[148]J. R. Hattrick-Simpers *et al.*, ACS Comb. Sci. **21**, 350 (2019).
[149]F. Bernardini, V. Fiorentini, and D. Vanderbilt, Phys. Rev. B **56**, R10024 (1997).
[150]E. T. Yu, X. Z. Dang, P. M. Asbeck, S. S. Lau, and G. J. Sullivan, J. Vac. Sci. Technol. B **17**, 1742 (1999).
[151]K. Shimada, T. Sota, and K. Suzuki, J. Appl. Phys. **84**, 4951 (1998).
[152]M. Feneberg and K. Thonke, J. Phys. Condens. Matter **19**, 26 (2007).
[153]F. Martin, P. Muralt, M.-A. Dubois, and A. Pezous, J. Vac. Sci. Technol. A **22**, 361 (2004).
[154]K. Tonisch, V. Cimalla, C. Foerster, H. Romanus, O. Ambacher, and D. Dontsov, Sens. Actuators A Phys. **132**, 658 (2006).
[155]M. Strassburg, J. Senawiratne, N. Dietz, U. Haboeck, A. Hoffmann, V. Noveski, R. Dalmau, R. Schlesser, and Z. Sitar, J. Appl. Phys. **96**, 5870 (2004).
[156]E. Iborra, J. Olivares, M. Clement, L. Vergara, A. Sanz-Hervás, and J. Sangrador, Sens. Actuators A Phys. **115**, 501 (2004).
[157]A. Ababneh, U. Schmid, J. Hernando, J. Sánchez-Rojas, and H. Seidel, Mater. Sci. Eng. B **172**, 253 (2010).
[158]N. Takeuchi, Phys. Rev. B **65**, 045204 (2002).
[159]A. Alsaad and A. Ahmad, Eur. Phys. J. B Condens. Matter Complex Syst. **54**, 151 (2006).
[160]F. Tasnádi, B. Alling, C. Höglund, G. Wingqvist, J. Birch, L. Hultman, and I. A. Abrikosov, Phys. Rev. Lett. **104**, 137601 (2010).
[161]S. Fichtner, N. Wolff, F. Lofink, L. Kienle, and B. Wagner, J. Appl. Phys. **125**, 114103 (2019).
[162]S. Liu, K. Chang, S. Mráz, X. Chen, M. Hans, D. Music, D. Primetzhofer, and J. M. Schneider, Acta Mater. **165**, 615 (2019).
[163]Y. Iwazaki, T. Yokoyama, T. Nishihara, and M. Ueda, Appl. Phys. Express **8**, 061501 (2015).
[164]C. Tholander, F. Tasnádi, I. A. Abrikosov, L. Hultman, J. Birch, and B. Alling, Phys. Rev. B **92**, 174119 (2015).
[165]Y.-W. Fang, C. A. J. Fisher, A. Kuwabara, X.-W. Shen, T. Ogawa, H. Moriwake, R. Huang, and C.-G. Duan, Phys. Rev. B **95**, 014111 (2017).
[166]K. R. Talley, J. Mangum, C. L. Perkins, R. Woods-Robinson, A. Mehta, B. P. Gorman, G. L. Brennecka, and A. Zakutayev, Adv. Electron. Mater. **5**, 1900214 (2019).
[167]S. Manna, P. Gorai, G. L. Brennecka, C. V. Ciobanu, and V. Stevanović, J. Mater. Chem. C **6**, 11035 (2018).
[168]F. Liu *et al.*, Nat. Commun. **7**, 12357 (2016).
[169]M. Wu and X. C. Zeng, Nano Lett. **16**, 3236 (2016).
[170]C. Cui, F. Xue, W.-J. Hu, and L.-J. Li, Npj 2D Mater. Appl. **2**, 18 (2018).
[171]L. Ward, A. Agrawal, A. Choudhary, and C. Wolverton, Npj Comput. Mater. **2**, 16028 (2016).
[172]K. Alberi *et al.*, J. Phys. D Appl. Phys. **52**, 13001 (2018).
[173]K. Ryan, J. Lengyel, and M. Shatruk, J. Am. Chem. Soc. **140**, 10158 (2018).
[174]Q. M. Zhang, W. Y. Pan, and L. E. Cross, J. Appl. Phys. **63**, 2492 (1988).
[175]Z. Huang and R. W. Whatmore, Rev. Sci. Instrum. **76**, 123906 (2005).
[176]S. Shetty, J. I. Yang, J. Stitt, and S. Trolier-Mckinstry, J. Appl. Phys. **118**, 174104 (2015).